

# The modelling and simulation of high-frequency electronic circuits<sup>‡</sup>

Thomas J. Brazil<sup>\*,†</sup>

*School of Electrical, Electronic and Mechanical Engineering, University College Dublin, Dublin 4, Ireland*

## SUMMARY

This paper provides an overview of progress in selected topics related to the modelling and simulation of high-frequency electronic circuits. There are several specific features of this regime that distinguish it from more conventional electronic analysis; however, here we will just emphasize two: firstly, the durable value, and yet the intrinsic limitations, of the circuit paradigm in representing the physical behaviour of high-frequency electronic devices, and secondly, the challenge of efficiently representing frequency-domain linear data in general non-linear transient simulation. Copyright © 2007 John Wiley & Sons, Ltd.

Received 14 June 2007; Revised 25 June 2007

KEY WORDS: Nonlinear; Modelling; Simulation; Microwave; Convolution

## 1. INTRODUCTION

The title of this paper immediately invites the question of what is meant by ‘high frequency’. In broad terms, the following discussion on modelling and simulation will refer to signals having significant spectral energy in the microwave or millimetre-wave band. These signals may be analogue carriers, perhaps modulated in a complex manner with digital data, or perhaps they may be broadband gigabit-speed digital signals. As a doctoral student and later colleague of Sean Scanlan, the author developed a life-long interest in the intriguing problems created in the high-frequency domain by the fusion of device physics and electromagnetic (EM) behaviour, in particular where circuit theory insights may provide simplified but useful descriptions of behaviour as a basis for subsequent numerical solution. The applications to practical design are numerous and of high commercial importance, ranging from advanced physical layer design of wireless

\*Correspondence to: Thomas J. Brazil, School of Electrical, Electronic and Mechanical Engineering, University College Dublin, Dublin 4, Ireland.

<sup>†</sup>E-mail: tom.brazil@ucd.ie

<sup>‡</sup>Dedicated to Professor Seán Scanlan on the occasion of his 70th birthday.

Contract/grant sponsor: Science Foundation Ireland

communications systems to the so-called ‘signal integrity’ problems limiting the achievable speeds in high-performance digital electronics.

Inevitably, this is a very large subject, and the topics that follow represent just a selection of the great deal of progress that has taken place over the past three or four decades. The interested reader is referred to many excellent sources and reviews as a basis for further reading [1–3].

In order to focus and structure the discussion, two specific themes will be considered in more detail. The first relates to high-frequency transistor modelling, particularly in the general case of non-linear operation, while the second deals with the challenges posed by simulating complex non-linear systems with very general kinds of signals, where part of the system (consisting of the transistors) is more naturally described in the time domain while another part (consisting of the distributed circuits) is much more conveniently described in the frequency domain. Some examples will also be provided.

## 2. CIRCUIT-LEVEL MODELLING OF HIGH-FREQUENCY TRANSISTORS

It is clear that non-linear active device modelling continues to be of major importance across a wide range of electronic applications. In particular, we concentrate here on FET-type devices which are widely used in analogue or mixed-signal high-frequency applications [4]. The early GaAs MESFET technology has now been largely supplanted by the more complex but technically superior pseudomorphic HEMT (PHEMT) in many microwave applications [5]. Simultaneously, from the lower-frequency side, deep sub-micron CMOS technology has made major advances into the microwave and even millimetre band, while extremely high power levels may be obtained with LDMOS or newer wide band gap devices using material systems such as gallium nitride [6]. Although different physical processes are invoked by these devices, they are all fundamentally FETs and share many common non-linear modelling issues.

In practice, the modelling of a given device requires a representation of the environment separating the active core (or ‘intrinsic’) device from a set of recognizable ports at which the world outside the device (viewed as a component) may be said to begin. In power devices, this requires a thermal as well as an electrical description. Often (linear) lumped and/or distributed circuit elements are used in both domains, but determining the most effective topology and devising procedures—often experimental—for the identification of specific elements are far from trivial at high frequencies and may require a good deal of insight and experience.

The most fundamental approach to the modelling of the core intrinsic device involves the formulation of a set of partial differential equations as a boundary-value problem in space and time incorporating the basic transport, relaxation and quantum phenomena. In very small-scale high-frequency devices, standard drift-diffusion approximations may no longer be adequate resulting in more complex formulations such as those based on hydrodynamic models [7]. While providing great insight, direct physics-based analysis remains too complex from an engineering point of view for many routine applications, and by far the most widespread approach to high-frequency modelling relies on creating ‘compact’ equivalent circuit models which seek to retain the essential internal physical dynamics while achieving the great advantage of a natural compatibility with general-purpose circuit simulators. It must be stressed that there is no automatic reason why the space of non-linear representations generated by any topological arrangement of a finite number of standard circuit elements (even if permitted to be non-linear in some set of controlling variables) should encompass all the rich dynamical behaviour of complex high-frequency transistors. Indeed,

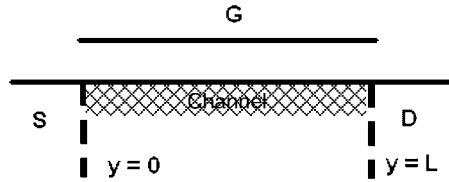


Figure 1. Simplified representation of FET physical structure.

the simple example of the exact small-signal analysis of a forward-biased PN junction exposes the fact that this is not true even in a very simple device structure. It is a remarkable fact that equivalent circuit models have proven to work very well for many purposes, although some of their inherent simplifications are becoming more apparent as operating frequencies increase.

In order to illustrate the power but also the limitations of this approach, we begin with a generic FET structure as shown in Figure 1, where the current in an existing or induced conducting channel connecting the source and drain is controlled by the voltage at the gate. A simple physical model for this structure may be developed (assuming 1-D flow, negligible diffusion, linear mobility, etc.) with  $Q_n(y, t)$  representing the instantaneous (electron) channel charge per unit surface area at a location  $y \in [0, L]$  in a device of width  $W$ . The channel particle current  $i_D(y, t)$  may be written as

$$i_D(y, t) = \mu^* \cdot Q_n(y, t) \cdot \frac{\partial v(y, t)}{\partial y} \quad (1)$$

where  $\mu^*$  is an effective mobility and  $v(y, t)$  is the local potential. The continuity equation provides a further connecting relationship:

$$\frac{\partial Q_n(y, t)}{\partial t} = - \frac{\partial v(y, t)}{\partial y} \quad (2)$$

Various controlling laws relating  $Q_n(y, t)$  to the gate voltage and other parameters may be developed depending on the physics of a particular device. For example, motivated by detailed physical modelling we have found a compact single-function formulation that works very well for bulk and SOI RF MOS devices [8].

Equations (1) and (2) show that particle and displacement currents are closely intermingled in the channel; however, most equivalent circuit models effectively assume that the operating frequencies are sufficiently low so that the RHS of Equation (2) may be set to zero. This is the ‘quasi-static’ approximation which has the consequence that change in gate voltage causes a simultaneous change in voltage at all points in the channel. It is natural then to describe the particle current in the channel by a non-linear voltage-dependent current source such as  $i_{DS}(v_{GS}, v_{DS})$  and to separate the displacement current into two parts, one forming a path between the (internal) gate and source and the other between the internal gate and drain. Associated with these are (non-linear) capacitances  $C_{GS}(v_{GS}, v_{GD})$  and  $C_{GD}(v_{GS}, v_{GD})$ , respectively. This leads to the familiar ‘ $\Pi$ ’ architecture at the core of most FET circuit models as shown in Figure 2. Detailed analysis shows that a first-order allowance for non-quasi-static (NQS) behaviour may be made by inserting (non-linear) resistances in series with each capacitor, and this is often done in the more advanced high-frequency FET models of this kind.

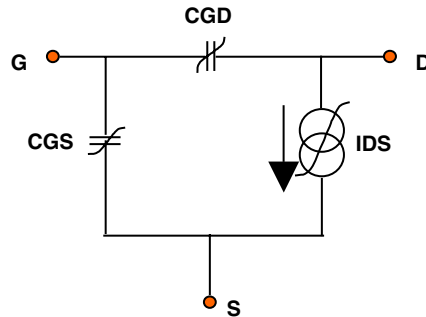


Figure 2. Core elements of intrinsic FET equivalent circuit model.

While a reasonably successful approach, ultra-high operating frequencies into the millimetre wave or beyond cause severe NQS effects that challenge conventional equivalent circuit models. One approach to overcoming this problem is through using a segmented channel representation based on Equations (1) and (2). This has been shown to work successfully well into millimetre wave in static, small-signal and highly non-linear operations [8].

A more subtle difficulty related to the model structure adopted in Figure 2 relates to what is often termed as charge conservation. Most circuit simulators use some variation of nodal analysis and can only deal with capacitive non-linearity through charge functions, which are considered to be ‘state variables’. Hence, if a nodal charge is expressed as a function of multiple voltages, the charge must return to the same value when exercised through any closed dynamic path in the voltage space. Charge is then said to be ‘conserved’.

This can be a confusing and sometimes even controversial area in the context of FET modelling, but it is argued here that from a physical point of view, the *only* charge that must be conserved is the total (single) charge on the gate electrode. This charge may be written as a function of the independent intrinsic terminal voltages as  $Q_G(v_{GS}(t), v_{GD}(t))$ . A difficulty is that this charge cannot be determined directly from measurement, only indirectly, for example, *via* small-signal capacitances, which can be identified with the first partial derivatives of the total charge. These appear as  $C_{GS}$  and  $C_{GD}$  in the model of Figure 2. Taking the total differential of  $Q_G$ :

$$\begin{aligned} dQ_G &= \frac{\partial Q_G}{\partial v_{GS}} dv_{GS} + \frac{\partial Q_G}{\partial v_{GD}} dv_{GD} \\ &= C_{GS} dv_{GS} + C_{GD} dv_{GD} \end{aligned} \quad (3)$$

It can be shown from vector algebra that these capacitances imply a conservative underlying total charge if they satisfy the constraint:

$$\frac{\partial C_{GS}}{\partial v_{GD}} = \frac{\partial C_{GD}}{\partial v_{GS}} \quad (4)$$

This can be readily tested in the context of a model such as that of Figure 2. For properly extracted data, it is found that Equation (4) will be generally well obeyed. The main error will be below the ‘knee’ region, where the basic validity of the  $\Pi$ -model topology is more questionable. Of course,

measurement uncertainty, parasitic extraction errors as well as the limitations of the topology mean that perfect charge conservation can never be obtained in practice.

If a simulator could act directly on non-linear capacitance functions, there would be little more to add. However, the commonly used simulators cannot act directly on non-linear capacitance but require a (conservative) charge formulation instead. This requires that instead of  $C_{GS}$ , for example, a new  $Q_{GS}(v_{GS}, v_{DS})$  must be constructed which is conservative, and, separately, a  $Q_{GD}(v_{GS}, v_{DS})$  must be obtained which meets the same criterion. While it is reasonable that the *sum* of  $Q_{GS}$  and  $Q_{GD}$  should be conservative, there is no reason physically why they should be so separately. However, in an effort to meet the demands of the simulator, it is not uncommon to introduce ‘transcapacitances’ into the G–S and G–D branches to force the conservation requirement on the separate charge functions [9]. Not surprisingly, this can have unintended negative consequences: energy conservation may be violated, and the large-signal model may not (as would be expected) correctly asymptote to a correct small-signal model as the signal amplitude is reduced. It is possible with some ingenuity to use circuit structures that enable a nodally based simulator to deal directly with non-linear capacitance—for example, the circuit in Figure 3 may be employed.

While the circuit model of Figure 2 retains at least some connection with the physical structure, ‘table-based’ models use a more abstract formulation as shown in Figure 4. In principle, large amounts of experimental data may be used to construct the ‘tables’ from which values of the various non-linear parameters may be found by interpolation. Charge conservation means that this structure requires the use of transcapacitances. This is a rather restricted topology that forces a strict separation into particle and displacement current directly at each node; however, it has the considerable merit of being in a form ideally suited to high-frequency microwave simulation using the harmonic balance technique and its variants. The so-called ‘relaxation times’ [10] may be introduced to allow more complex descriptions of dynamic behaviour.

A further difficulty in high-frequency modelling, especially with FETs using compound semiconductors, is that the channel current behaviour at high frequencies can be distinctly different from that observed at DC or low frequencies, due to dynamical influences associated with channel or surface traps. A variety of modelling strategies has been developed to take account of such ‘dispersion’ phenomena. Figure 5 shows the structure of an advanced non-linear device model which includes additional elements in the drain path to account for such dispersion effects. In addition to the NQS-based resistances in series with capacitances mentioned earlier, there are also diode branches to account for possible forward conduction of the Gate Schottky [11]. A two-pole thermal RC equivalent circuit (not shown) is linked to this electrical model to complete the description.

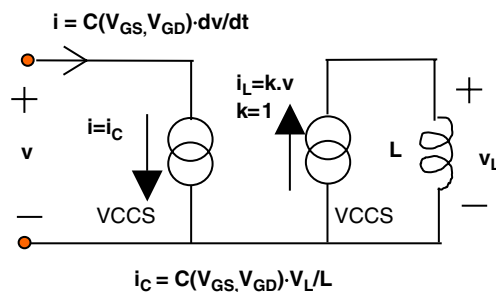


Figure 3. Using circuit elements to allow non-charge-based implementation of non-linear capacitance.

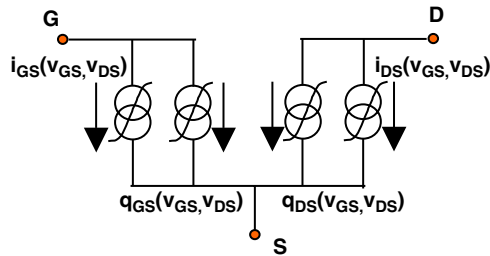


Figure 4. Basic topology of table-based FET non-linear model.

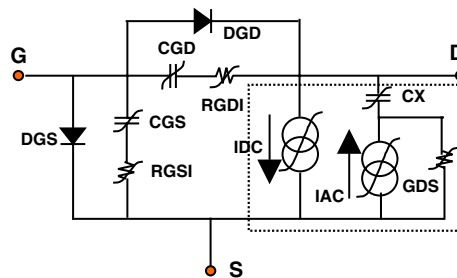


Figure 5. Advanced FET equivalent circuit model including additional elements to model dispersion in drain current.

### 3. LINEAR TRANSIENT SIMULATION WITH FREQUENCY-DOMAIN DATA

While device modelling and parameter extraction play a significant role in high-frequency design, a further challenge is posed by the predominantly EM or distributed nature of the external circuit environment at these frequencies. To some extent this can be accommodated by adding additional circuit elements, leading, for example, to the kind of quite complex parasitic networks often used for modelling a package or a similar component. Where very distinct distributed behaviour becomes evident, individual or multiple coupled transmission lines may be used to assist effective circuit-level modelling, although these may also show significant loss and dispersion. Beyond this, however, an efficient circuit equivalent can be difficult to find and it may be more effective to describe a component or subsystem (such as a spiral inductor or antenna) just through tabulated  $S$ -parameter data in the frequency domain, perhaps obtained from separate EM simulation. The classical microwave simulation challenge then presents itself: it is clear that the kind of device circuit model described in Section 2 naturally leads to a mathematical description in terms of a set of ordinary integro-differential equations in the time domain, whereas, as just noted, the environment external to these devices is usually most conveniently described in the frequency domain.

Harmonic balance (HB) and its many variants have evolved in response to this situation and is particularly suited to direct computation of the periodic, steady-state response of such a system when excited by a relatively small number of tones that are commensurate in frequency [12]. It does this usually by assuming a vector of finite-harmonic voltage signals at a set of interface ports

between both domains, and then determining the associated unknown complex amplitudes at each harmonic by iteratively ‘balancing’ the resulting currents in both frequency and time domains. A significant extension to this basic concept has been ‘envelope transient,’ in which each individual harmonic is further assumed to be modulated by a (narrow-band) complex baseband signal [13, 14]. For example, assuming the fundamental frequency to be  $\omega_0$ , then the voltage at the ‘ $i$ ’ port is described as

$$v^{(i)} = \sum_{k=-K}^{+K} V_k^{(i)} \cdot e^{jk\omega_0 t} \quad (5)$$

A time-domain solution is then performed consisting of a sequence of HB solutions at each time step. However, the most critical point is that the transient analysis time step is determined by the modulation waveform, not by the high-frequency tone(s). Some modifications to standard HB are then required. For example, a linear capacitor  $C$  at port ‘ $i$ ’ now returns a  $k$ th harmonic current component given by

$$I_k^{(i)} = jk\omega_0 C \cdot V_k^{(i)} + C \cdot \frac{d(V_k^{(i)}(t))}{dt} \quad (6)$$

The method relies on each signal having a reasonably sparse spectral structure and is particularly suited to non-linear analysis with digitally modulated carriers.

In the remainder of this section, we focus on an alternative approach to this problem that in principle offers most generality but in practice tends to be relatively little used, namely that based on numerical convolution [15, 16]. This approach suffers from something of a bad image being associated with difficult numerical procedures and long execution times as the duration of solution grows. If properly performed, however, as will be shown in the following, these difficulties can be largely overcome resulting in a method of high-frequency simulation that is powerful, accurate and very general.

The fundamental operation of convolution is well known. If a linear, time-invariant, causal one-port network with a driving point admittance  $Y(f)$  and an admittance impulse response  $h_Y(t)$  is excited by a finite-energy voltage  $v(t)$ ,  $t \in [0, \infty[$ , then the instantaneous current response may be found as

$$\begin{aligned} i(t) &= \int_0^t h_Y(\tau) \cdot v(t - \tau) d\tau = \int_0^t v(\tau) \cdot h_Y(t - \tau) d\tau \\ h_Y(t) &= \int_{-\infty}^{+\infty} Y(f) \cdot e^{j2\pi ft} \end{aligned} \quad (7)$$

A simple first observation is that if the impulse response duration can be assumed to be finite and reasonably short ( $T$ ), then the computational effort associated with the integrals initially grows with time but then stays fixed for any solution interval beyond  $T$ . Even so, the statement is often encountered in the literature that the computational effort in convolution is always proportional to the total solution period.

In approaching Equation (7) numerically, a key decision is whether to treat impulse response values  $h_Y(i \cdot \Delta t)$  as samples of an underlying continuous function (as is usually the case), or instead to view these samples as ‘weights’ or as a true discrete-time function. This is connected with another basic issue arising from the fact that the given frequency-domain data is often only available or are only of interest over a finite frequency band, whereas the calculation of Equation (7) in principle

requires knowledge of all frequencies. A common approach is to ‘window’ the given frequency-domain data to force them to be zero valued outside the known region, which, besides introducing distortion, immediately implies the former interpretation of  $h_Y(i \cdot \Delta t)$ . An alternative method is to seek to form the periodic extension of the known (Hermitean) frequency-domain data, which can then be represented by a set of (real valued) truly discrete-time samples in the time domain as a form of reverse-Fourier series, consistent with the second interpretation. However, any direct attempt at periodic extension will usually lead to severe Gibbs phenomena due to discontinuities at the boundary frequencies. We now describe briefly the successful development of a solution to this problem, with the objective of representing in discrete time all of the  $S$ -parameters of a completely arbitrary  $N$ -port linear, time-invariant network that are available from DC up to some maximum frequency of interest  $f_m$ . The use of scattering or  $S$ -parameters is not essential but being bounded in magnitude they appear generally to represent a better choice.

We assume a given (Hermitean)  $S$ -parameter function  $S_{ij}(f) = (S_{ij}^r(f) + j \cdot S_{ij}^i(f))$ , either of the reflection or transmission type which is referred to as  $G_0$  and specified at  $(N + 1)$  equally spaced tabulated values of  $f \in [0, f_m]$  with interval  $\Delta f$ . As already noted, a direct periodic extension of the given data beyond the known range  $[-f_m, f_m]$  will, in general, introduce major complex-valued discontinuities at each boundary frequency. If it were then attempted to convert a function of this kind into the time domain, the resulting impulse response would be of very long duration and/or would have very poor interpolation properties back into the frequency domain between the original data points. Consider now the new function:

$$F_{ij}(f) = [S_{ij}(f) - K] \cdot e^{-j\omega\tau} \quad (8)$$

where  $K$  and  $\tau$  are real numbers, and  $\tau \in [0, (\frac{1}{2}f_m)]$ . These numbers should be chosen to satisfy the following two simultaneous conditions:

- (1)  $\text{Im}\{F_{ij}(f_m)\} = 0.0$ . For a Hermitean  $S_{ij}$  this is sufficient to avoid a discontinuity in  $F_{ij}$  at  $f = f_m$ .  $F_{ij}$  is thus continuous and periodic in a complex-valued sense and may be represented efficiently by a discrete-time sequence of impulse response weights separated by  $\Delta t_{ir} = (\frac{1}{2}f_m)$ ;
- (2) The impulse response weight calculated as a result of condition (1) at time = 0 is forced to be exactly zero.

It can be shown that the procedure required to satisfy simultaneously conditions (1) and (2) reduces to determining a value of  $\tau$  in the range  $[0, (\frac{1}{2}f_m)]$  such that

$$\begin{aligned} \Delta f \cdot \left[ \sum_{i=1}^{N-1} 2\{S_{ij}^r(i\Delta f) - K\} \cos(\omega_m \cdot \tau) + S_{ij}^i(i\Delta f) \sin(\omega_m \cdot \tau) \right] + [S_{ij}^r(0) - K] \\ + [S_{ij}^r(f_m) - K] \cos(\omega_m \cdot \tau) + S_{ij}^i(f_m) \sin(\omega_m \cdot \tau) = 0 \end{aligned}$$

where

$$K = S_{ij}^r(f_m) - (S_{ij}^i(f_m) / \tan(\omega_m \cdot \tau)) \quad (9)$$

This is a straightforward numerical exercise in finding a bracketed root of an algebraic non-linearity.

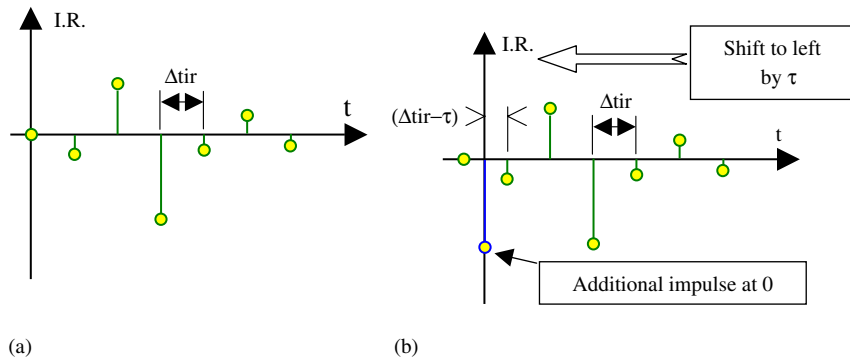


Figure 6. (a) Time-domain representation of periodic extension of  $F_{ij}(f)$  in Equation (8), satisfying both conditions (1) and (2). (b) Time-domain representation of scattering parameter  $S_{ij}(f)$  derived from response in (a).

The resulting time-domain representation of  $F_{ij}(f)$  may resemble that shown in Figure 6(a). However, our original objective was to obtain a discrete-time representation of the scattering parameter  $S_{ij}(f)$ . This is achieved as follows:

1. Remove the additional phase shift introduced by the exponential term in Equation (8). This corresponds to shifting the entire response in Figure 6(a) by an amount  $\tau$  to the left, i.e. in the direction of negative time, and explains the need for condition (2), since moving the first, zero-valued weight into the negative time region does not then lead to a violation of causality.
2. If  $K$  is non-zero, introduce an additional impulse at time 0 of value  $(K \cdot \Delta t_{ir})$ . The discrete-time representation of  $S_{ij}(f)$  is therefore as shown in Figure 6(b), potentially non-uniform adjacent to the origin, but uniform otherwise. Typically an order of 50–100 weights are sufficient to represent completely even quite complex frequency-domain behaviour.

Provided sufficient samples are taken up to some maximum frequency  $f_m$  (corresponding to the highest spectral energy of interest), the resulting discrete-time data can interpolate continuously and with very high accuracy between the original samples leading to high accuracy in transient analysis.

As an example, consider an ultra wide band (UWB) antenna using a defected ground structure designed to cover the 3.5–10-GHz band, as shown in Figure 7. The calculated reflection coefficient using commercial EM software is shown in Figure 8 (the experimental results obtained were close to those predicted, but are not included in the interests of clarity). Also shown are just eight individual samples of this response that were used to construct a discrete time-domain representation of the system using the above method resulting in the representation indicated in Figure 9. Padding with zeros and inverting back into the frequency domain, makes it possible to test the interpolation properties of this representation in the continuous frequency domain. The results, also shown in Figure 8, are smooth and very close to the original EM data over the full band. Obviously, more samples could be used to achieve even greater accuracy.

With the discrete-time IR record obtained, full transient analysis (linear or non-linear) is straightforward using numerical convolution. As a simple example, assume that the admittance function in Equation (7) earlier was represented in discrete time using this method. Assume further that a (constant) time step  $\Delta t$  is used that is a relatively large integer fraction ‘ $p$ ’ of the time interval

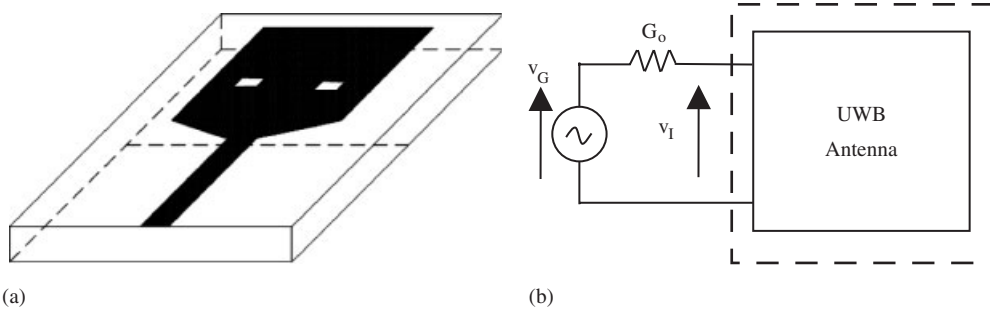


Figure 7. (a) Schematic of microstrip defected ground UWB antenna structure (substrate dielectric constant = 2.55) and (b) circuit schematic for transient analysis.

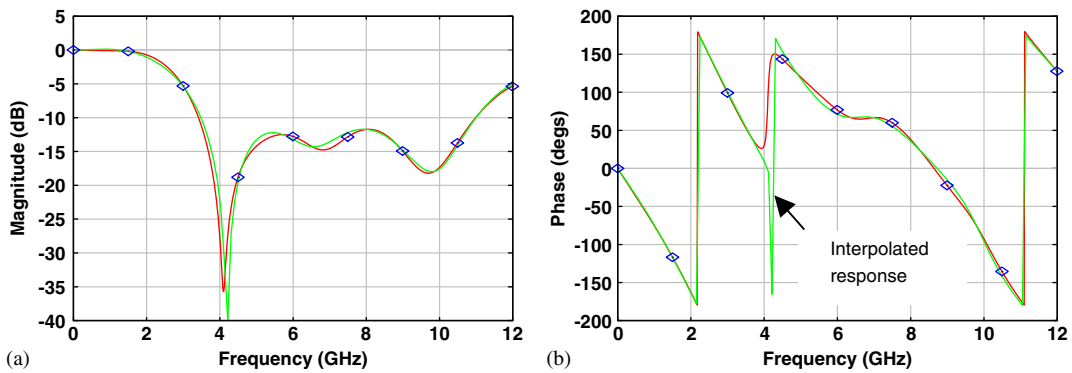


Figure 8. Reflection scattering parameter of the UWB antenna as a function of (a) frequency and (b) magnitude phases. Points indicate samples used to construct discrete-time impulse response. Interpolated and exact (EM) responses compared.

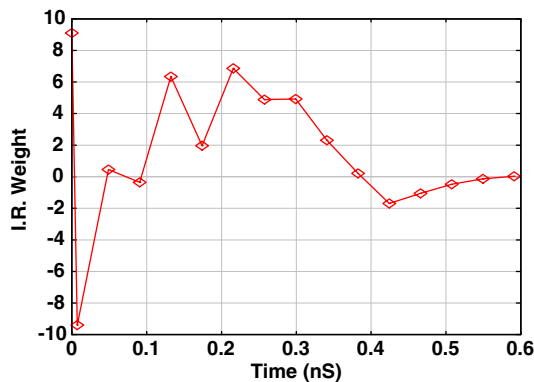


Figure 9. Discrete-time representation of reflection scattering parameter of the UWB antenna using frequency samples shown as points in Figure 8.

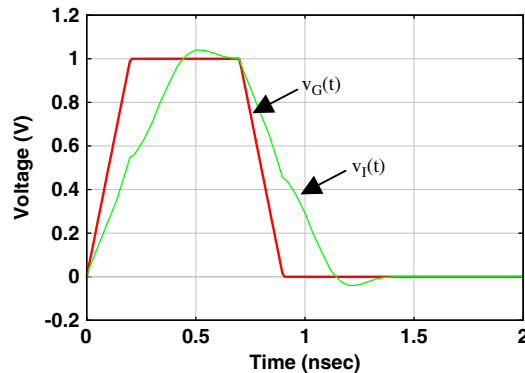


Figure 10. Pulse-transient response of the UWB antenna system in Figure 7(b) using discrete-time representation in Figure 9.

separating IR weights ( $\Delta t_{ir}$ ), and that the initial delay  $\tau$  is also an integer fraction ‘ $q$ ’ of the same interval, then the earlier convolution integral now becomes an exact (finite) summation:

$$i(k\Delta t) = \left[ h_Y(0) \cdot v(k\Delta t) + \sum_{n=1}^{2N-1} [h_Y(n) \cdot v((k - q - p \cdot (n - 1)) \cdot \Delta t)] \right] \cdot \Delta t_{ir}$$

Note that the convolution ‘integral’ is no longer a quadrature but a true sum-of-products calculation, and that also the duration of the convolution is limited by the relatively short length of the impulse response record. By arranging as in this case for the time step for transient simulation to be an integer fraction of the time intervals of the impulse response record, interpolation is avoided and excellent efficiency and dynamic range accuracy become possible.

The analysis based on a reflection scattering parameter is slightly more involved but similar in principle. For example, Figure 10 shows the input transient pulse response ( $v_I(t)$ ) of the antenna depicted in Figure 7 when calculated in this way. Numerous other tests have verified the high accuracy, generality and stability/robustness of this method of representing frequency-domain data.

#### 4. NON-LINEAR HIGH-FREQUENCY TRANSIENT SIMULATION

Using a combination of the advanced physically consistent non-linear device models as described in Section 2, together with the efficient and general technique for the representation of linear frequency-domain data as described in Section 3, a wide variety of complex signal excitation scenarios can be analysed in high-frequency applications.

As an example, Figure 11 shows a microwave amplifier with input and output matching networks containing lossy dispersive transmission lines. The PHEMT device used is modelled with an advanced electro-thermal model that includes the features described in Section 2. The frequency-domain linear blocks are represented in the manner outlined in Section 3. A full non-linear transient simulation is carried out using discrete-time convolution. Figure 12(a) shows the calculated steady-state spectrum of the output (load) voltage under single-tone sinusoidal operation at 5.8 GHz. It is

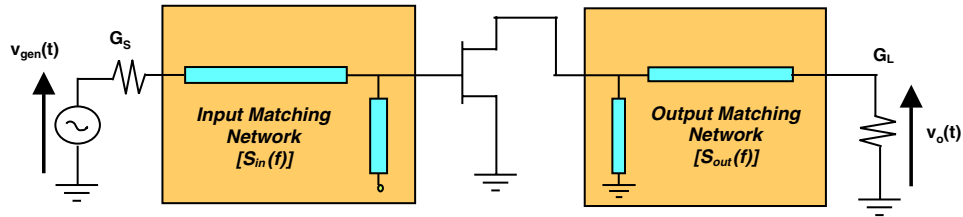


Figure 11. PHEMT amplifier incorporating non-linear device model as in Figure 5 and distributed matching/bias networks represented in discrete time.

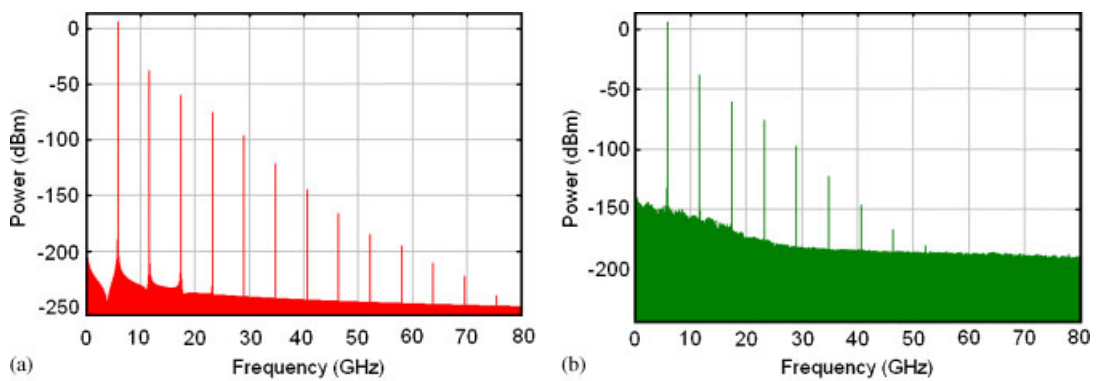


Figure 12. (a) Output voltage spectrum with single-tone input voltage at 5.8 GHz (amplitude = 2 V,  $V_{GS} = -0.2$  V,  $V_{DS} = 3.0$  V) and (b) as (a) with channel noise introduced directly as signal generator.

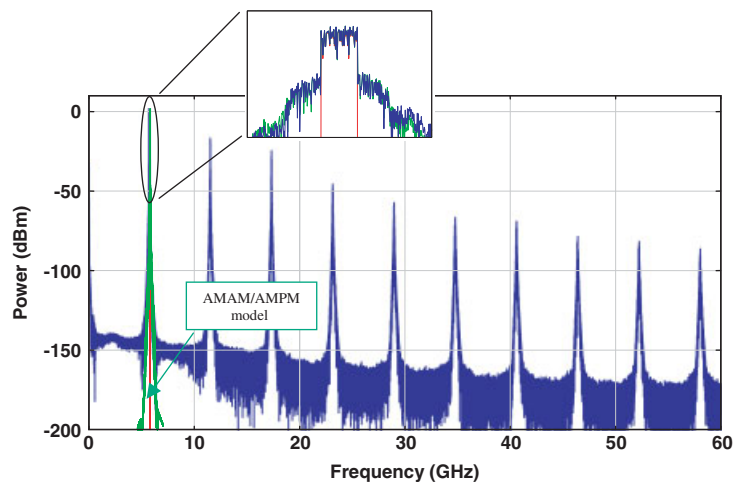


Figure 13. Broadband output voltage spectrum with 64-channel OFDM signal, each channel modulated with 64-level QAM. AMAM/AMPM behavioural model shown for comparison (in the first zone).

seen that a remarkable numerical dynamic range of the order of 200 dB can be achieved, which, for example, allows direct introduction of the FET channel noise into the simulation as a real random signal, allowing the full range of interactions of non-linearity and noise to be taken into account (Figure 12(b)).

Some results of a more demanding simulation condition are shown in Figure 13, where the input signal is now an OFDM waveform composed of 64 individual carriers centred at 5.8 GHz each separately modulated with a 64-level QAM modulation scheme. The output spectrum shown, although possessing an essentially zonal character, is very complex but the simulation techniques described earlier are easily capable of dealing with very strong non-linearity and broadband behaviour in this situation. The inset diagram shows closer details of the first zone response, where the results of an AMAM/AMPM-based behavioural model [17] are also included for comparison. These provide an independent verification of the accuracy of the simulation within the first zone region.

## 5. CONCLUSIONS

This paper has reviewed a selection of topics in the field of high-frequency modelling and simulation, which is of continuing and even growing strategic importance because of the rapid growth in wireless-based communications. While a comprehensive review was not possible in the space available, two key areas of enduring interest have been focussed on, one relating to high-frequency non-linear modelling and the other to representing general linear systems over a broadband in an effective way compatible with general non-linear simulation. It has been shown that with care, an efficient and general modelling and simulation environment can be created capable of supporting very challenging design tasks, involving signals with a very wide dynamic range operating over large bandwidth.

## ACKNOWLEDGEMENTS

This work was supported by an Investigator Award from Science Foundation Ireland. At a personal level, the author wishes to acknowledge his great debt to Sean Scanlan for his guidance and advice over many years, and his specific contributions to several of the ideas presented here.

## REFERENCES

1. Maas SM. *Nonlinear Microwave Circuits*. Artech House: Norwood, MA, 1988.
2. Rodrigues PJC. *Computer-aided Analysis of Nonlinear Microwave Circuits*. Artech House: Norwood, MA, 1998.
3. Pedro JC, Carvalho NB. *Intermodulation Distortion in Microwave and Wireless Circuits*. Artech House: Norwood, MA, 2003.
4. Aaen P, Plá JA, Wood J. *Modeling and Characterization of RF and Microwave Power FETs*. Cambridge University Press: Cambridge, MA, 2007.
5. Larson LE. Microwave device and circuit challenges for next generation wireless applications. *IEEE Topical Conference on Wireless Communication Technology*, Honolulu, HI, October 2003; 74–77.
6. Sheppard ST, Doverspike K, Pribble WL, Allen ST, Palmour JW, Kehias LT, Jenkins TJ. High-power microwave GaN/AlGaIn HEMT on semi-insulating silicon carbide substrates. *IEEE Electron Device Letters* 1999; **20**: 161–163.
7. Rudge PJ, Miles RE, Steer MB, Snowden CM. Investigation into intermodulation distortion in HEMTs using a quasi-2-D physical model. *IEEE Transactions on Microwave Theory and Techniques* 2001; **49**:2315–2321.

8. Burke DR, El Kaamouchi M, Vanhoenacker-Janvier D, Brazil TJ. DC and large-signal microwave MOSFET model applicable to partially-depleted, body-contacted SOI technology. *Proceedings of the 2007 IEEE MTT-S International Microwave Symposium*, Honolulu, HI, June 2007; 585–589.
9. Snider AD. Charge conservation and the transcapacitance element: an exposition. *IEEE Transactions on Education* 1995; **38**:376–379.
10. Daniels RR, Yang AT, Harrang JP. A universal large/small signal 3-terminal FET model using a nonquasi-static charge-based approach. *IEEE Transactions on Electron Devices* 1993; **40**:1723–1729.
11. Cojocaru VI, Brazil TJ. A scalable general-purpose model for microwave FETs including DC/AC dispersion effects. *IEEE Transactions on Microwave Theory and Techniques* 1997; **45**:2248–2255.
12. Kundert KS, White JK, Sangiovanni-Vincentelli A. *Steady-state Methods for Simulating Analog and Microwave Circuits*. Kluwer Academic Publishers: Boston, MA, 1990.
13. Brachtendorf HG, Welsch G, Laur R, Bunse-Gerstner A. Numerical steady-state analysis of electronic circuits driven by multi-tone signals. *Electrical Engineering* 1996; **79**:103–112.
14. Sharritt D. Method for simulating a circuit. US Patent 5588142, December 1996.
15. Brazil TJ. Causal-convolution—a new method for the transient analysis of linear systems at microwave frequencies. *IEEE Transactions on Microwave Theory and Techniques* 1995; **43**:315–323.
16. Brazil TJ. Highly accurate incorporation of frequency-domain data within linear and non-linear time-domain transient simulation. *Proceedings of the 2005 IEEE MTT-S International Microwave Symposium*, WE3D-1, Long Beach, CA, June 2005.
17. Pedro JC, Maas SA. A comparative overview of microwave and wireless power-amplifier behavioral modeling approaches. *IEEE Transactions on Microwave Theory and Techniques* 2005; **53**:1150–1163.